under- or over-estimated. Thus, we proposed time-averaged AUROC as a new evaluation index for the prediction efficiency of the CoxPH model, which will be a robust index.

Future prospects regarding clinical application of microarray technology

The MAQC project was initiated by the U.S. FDA, and the second phase (MAQC-II) is currently in progress [33]. Its aims are to assess the capabilities and limitations of microarray-based predictive models, and to reach a consensus for the development and validation of microarray-based predictive models for personalized medicine. Although reports from MAQC-II have not been published yet, their reports will have a great impact on finalizing a draft guideline of IVDMIA. Prior to finalizing the IVDMIA guideline by the U.S. FDA, the FDA have already cleared two microarray-based IVDMIA devices, MammaPrint™ and Pathwork Tissue Origin Test™. In addition, OncoTypeDX®, a RT-PCR-based IVDMIA, is widely used because health insurance companies have adopted it as a criterion for insurance payment. However, a microRNA-based IVDMIA device has not been developed and approved yet. MicroRNA can be detected even in formalin-fixed paraffin-embedded specimens [34], or remote fluid samples such as blood[35], because of their stability. Therefore, microRNAs are thought to be good biomarkers. The progress in this study will be fundamental for the future application of microRNA-microarray based IVDMIA into the clinical field. However, our prediction model was only internally validated. Therefore, prospective and external validation is necessary before it is introduced to put microRNA microarray into practical use.

Supporting Information

Description S1 Details of analysis procedures were described.
(DOC)

Figure S1 A heatmap and unsupervised clustergram of microRNA expression in tumor and non-tumor tissues of HCC patients. This heatmap represents an overview of microRNA expression profile. The microRNA expression data was centered by 2 directions (i.e., by genes and patients). Red, green, and black represent high, low, and intermediate microRNA expression. Blue and yellow bars on the top of the heatmap represent non-tumor, and tumor tissues.
(DOC)

Figure S2 Correlation between DNA chip and Taqman data for miR-96 expression. DNA chip expression data for miR-96 were validated by Taqman microRNA assay. DNAchip data and Taqman data were significantly correlated ($p<0.0001$). Left: x-axis: DNA chip data in a log2 scale, y-axis: Taqman data in an arbitrary log2 scale. Right: x-axis: DNA chip data in a log2 scale, y-axis: Taqman data in a log2 scale.
(DOC)

Table S1 Variables in clinicopathological dataset.
(DOC)

Table S2 Putative miR-96 target genes which expression is inversely correlated with miR-96 expression. *: these values are provided by TargetScan v.5.1, **: rank of total context score among 787 putative miR-96 target genes predicted by TargetScan. †: Pearson's correlation coefficients and p-values, ‡: Pubmed hit count using key words of gene symbol and "HCC, liver cancer, hepatocellular carcinoma", accessed on Dec 26, 2010.
(DOC)

Table S3 Significantly up-regulated microRNAs in HCC tumor tissues compared to non-tumor tissues. Up-regulated microRNAs with $p<0.01$ are listed. T-miRs, N-miRs: mean values of each T-miR and NmiR expression in log2 scale, fold change: expression ratio of each T-miR compared with corresponding N-miR, p-value: p-values of paired T-test. Order of microRNA is sorted by fold-change.
(DOC)

Table S4 Significantly down-regulated microRNAs in HCC tumor tissues compared to non-tumor tissues. Down-regulated microRNAs with $p<0.01$ are listed. T-miRs, N-miRs: mean values of each T-miR and NmiR expression in log2 scale, fold change: expression ratio of each T-miR compared with corresponding N-miR, p-value: p-values of paired T-test. Order of microRNA is sorted by fold-change.
(DOC)

Table S5 Differentially expressed microRNA compared with normal liver tissues. Differentially expressed microRNAs with $p<0.05$ are listed. T-miRs, N-miRs: mean values of each T-miR and NmiR expression in log2 scale, fold change: expression ratio of each T-miR or N-miR compared with normal liver tissues ($n=4$), p-value: p-values of unpaired T-test. The miR order is sorted by fold-change.
(DOC)

Table S6 Differentially expressed microRNAs depending upon HBV status. *: p-values of Student's T-test. Differentially expressed microRNAs with $p<0.05$ are listed.
(DOC)

Table S7 Differentially expressed microRNAs depending upon HCV status. * p-values of Student's T-test. Differentially expressed microRNAs with $p<0.05$ are listed.
(DOC)

Table S8 Differentially expressed microRNAs depending upon cellular grade. *: p-values of one-way ANOVA test. Differentially expressed microRNAs with $p<0.05$ are listed.
(DOC)

Table S9 Recurrence related microRNAs in HBV-positive cases. Univariate Cox proportional hazard model identified microRNAs associated with poor (red) and better (blue) recurrent outcome, respectively. Top-twenty significant microRNAs with p-value <0.05 are listed. MicroRNAs (displayed in red) which hazard ratio is greater than 1 were correlated with frequent recurrence, and are potential oncomiRs. In contrast, microRNAs (shown in blue) with hazard ratio less than 1 were associated with good recurrence-free survivals, and would be a tumor-suppressor miRs.
(DOC)

Table S10 Recurrence related microRNAs in HCV-positive cases. Univariate Cox proportional hazard model identified microRNAs associated with poor (red) and better (blue) recurrent outcome, respectively. Top-twenty significant microRNAs with p-value <0.05 are listed. MicroRNAs (displayed in red) which hazard ratio is greater than 1 were correlated with frequent recurrence, and are potential oncomiRs. In contrast, microRNAs (shown in blue) with hazard ratio less than 1 were associated with good recurrence-free survivals, and would be a tumor-suppressor miRs.
(DOC)

Table S11 Recurrence related microRNAs in hapatitis virus-negative cases. Univariate Cox proportional hazard model identi-

fied microRNAs associated with poor (red) and better (blue) recurrent outcome, respectively. Top-twenty significant microRNAs with p-value <0.05 are listed. MicroRNAs (displayed in red) which hazard ratio is greater than 1 were correlated with frequent recurrence, and are potential oncomiRs. In contrast, microRNAs (shown in blue) with hazard ratio less than 1 were associated with good recurrence-free survivals, and would be a tumor-suppressor miRs.
(DOC)

Table S12 Recurrence related microRNAs in grade 1–2 HCC cases. Univariate Cox proportional hazard model identified microRNAs associated with poor (red) and better (blue) recurrent outcome, respectively. Top-twenty significant microRNAs with p-value <0.05 are listed. MicroRNAs (displayed in red) which hazard ratio is greater than 1 were correlated with frequent recurrence, and are potential oncomiRs. In contrast, microRNAs (shown in blue) with hazard ratio less than 1 were associated with good recurrence-free survivals, and would be a tumor-suppressor miRs.
(DOC)

Acknowledgments

We thank Ms. Takako Murai and Ms. Chizuko Hirano for their technical assistance, and Ms. Sawako Okamoto for proofreading this article.

Author Contributions

Conceived and designed the experiments: FS EH. Performed the experiments: FS KK AM S. Tsuchiya. Analyzed the data: FS AM TF. Contributed reagents/materials/analysis tools: FS EH S. Takizawa GT SU KS. Wrote the paper: FS EH.

References

1. Stewart B, Kleihues P (2003) World Cancer Report. Lyon: IARC Press.
2. Akriviadis EA, Llovet JM, Efremidis SC, Shouval D, Canelo R, et al. (1998) Hepatocellular carcinoma. Br J Surg 85: 1319–1331.
3. El-Serag HB, Mason AC (1999) Rising incidence of hepatocellular carcinoma in the United States. N Engl J Med 340: 745–750.
4. Taylor-Robinson SD, Foster GR, Arora S, Hargreaves S, Thomas HC (1997) Increase in primary liver cancer in the UK, 1979–94. Lancet 350: 1142–1143.
5. Mazzaferro V, Regalia E, Doci R, Andreola S, Pulvirenti A, et al. (1996) Liver transplantation for the treatment of small hepatocellular carcinomas in patients with cirrhosis. N Engl J Med 334: 693–699.
6. Figueras J, Jaurrieta E, Valls C, Ramos E, Serrano T, et al. (2000) Resection or transplantation for hepatocellular carcinoma in cirrhotic patients: outcomes based on indicated treatment strategy. J Am Coll Surg 190: 580–587.
7. Michel J, Suc B, Montpeyroux F, Hachemanne S, Blanc P, et al. (1997) Liver resection or transplantation for hepatocellular carcinoma? Retrospective analysis of 215 patients with cirrhosis. J Hepatol 26: 1274–1280.
8. Taura K, Ikai I, Hatano E, Yasuchika K, Nakajima A, et al. (2007) Influence of coexisting cirrhosis on outcomes after partial hepatic resection for hepatocellular carcinoma fulfilling the Milan criteria: an analysis of 293 patients. Surgery 142: 685–694.
9. Ito T, Takada Y, Ueda M, Haga H, Maetani Y, et al. (2007) Expansion of selection criteria for patients with hepatocellular carcinoma in living donor liver transplantation. Liver Transpl 13: 1637–1644.
10. Bartel DP (2004) MicroRNAs: genomics, biogenesis, mechanism, and function. Cell 116: 281–297.
11. Griffiths-Jones S (2004) The microRNA Registry. Nucleic Acids Res 32: D109–111.
12. Zamore PD, Haley B (2005) Ribo-gnome: the big world of small RNAs. Science 309: 1519–1524.
13. Kim VN, Nam JW (2006) Genomics of microRNA. Trends Genet 22: 165–173.
14. Lagos-Quintana M, Rauhut R, Lendeckel W, Tuschl T (2001) Identification of novel genes coding for small expressed RNAs. Science 294: 853–858.
15. Tsuchiya S, Okuno Y, Tsujimoto G (2006) MicroRNA: biogenetic and functional mechanisms and involvements in cell differentiation and cancer. J Pharmacol Sci 101: 267–270.
16. John B, Enright AJ, Aravin A, Tuschl T, Sander C, et al. (2004) Human MicroRNA targets. PLoS Biol 2: e363.
17. Lu J, Getz G, Miska EA, Alvarez-Saavedra E, Lamb J, et al. (2005) MicroRNA expression profiles classify human cancers. Nature 435: 834–838.
18. Ye QH, Qin LX, Forgues M, He P, Kim JW, et al. (2003) Predicting hepatitis B virus-positive metastatic hepatocellular carcinomas using gene expression profiling and supervised machine learning. Nat Med 9: 416–423.
19. Lee JS, Chu IS, Heo J, Calvisi DF, Sun Z, et al. (2004) Classification and prediction of survival in hepatocellular carcinoma by gene expression profiling. Hepatology 40: 667–676.
20. Iizuka N, Hamamoto Y, Oka M (2004) Predicting individual outcomes in hepatocellular carcinoma. Lancet 364: 1837–1839.
21. Hoshida Y, Villanueva A, Kobayashi M, Peix J, Chiang DY, et al. (2008) Gene expression in fixed tissues and outcome in hepatocellular carcinoma. N Engl J Med 359: 1995–2004.
22. Budhu A, Jia HL, Forgues M, Liu CG, Goldstein D, et al. (2008) Identification of metastasis-related microRNAs in hepatocellular carcinoma. Hepatology 47: 897–907.
23. Meng F, Henson R, Wehbe-Janek H, Ghoshal K, Jacob ST, et al. (2007) MicroRNA-21 regulates expression of the PTEN tumor suppressor gene in human hepatocellular cancer. Gastroenterology 133: 647–658.
24. Ito T, Tanaka E, Kadowaki T, Kan T, Higashiyama M, et al. (2007) An ultrasensitive new DNA microarray chip provides gene expression profiles for preoperative esophageal cancer biopsies without RNA amplification. Oncology 73: 366–375.
25. Sato F, Tsuchiya S, Terasawa K, Tsujimoto G (2009) Intra-platform repeatability and inter-platform comparability of microRNA microarray technology. PLoS One 4: e5540.
26. Liver Cancer Study Group of Japan a (2000) The General Rules for the Clinical and Pathological Study of Primary Liver Cancer. Tokyo: Kanehara & Co., Ltd.
27. Centeno BA, Enkemann SA, Coppola D, Huntsman S, Bloom G, et al. (2005) Classification of human tumors using gene expression profiles obtained after microarray analysis of fine-needle aspiration biopsy samples. Cancer 105: 101–109.
28. Bolstad BM, Irizarry RA, Astrand M, Speed TP (2003) A comparison of normalization methods for high density oligonucleotide array data based on variance and bias. Bioinformatics 19: 185–193.
29. Utsunomiya T, Shimada M, Imura S, Morine Y, Ikemoto T, et al. (2010) Molecular signatures of noncancerous liver tissue can predict the risk for late recurrence of hepatocellular carcinoma. J Gastroenterol 45: 146–152.
30. Simon F, Bockhorn M, Praha C, Baba HA, Broelsch CE, et al. (2010) Deregulation of HIF1-alpha and hypoxia-regulated pathways in hepatocellular carcinoma and corresponding non-malignant liver tissue-influence of a modulated host stroma on the prognosis of HCC. Langenbecks Arch Surg.
31. Ladeiro Y, Couchy G, Balabaud C, Bioulac-Sage P, Pelletier L, et al. (2008) MicroRNA profiling in hepatocellular tumors is associated with clinical features and oncogene/tumor suppressor gene mutations. Hepatology 47: 1955–1963.
32. Guttilla IK, White BA (2009) Coordinate regulation of FOXO1 by miR-27a, miR-96, and miR-182 in breast cancer cells. J Biol Chem 284: 23204–23216.
33. FDA US MicroArray Quality Control (MAQC). http://www.fda.gov/ScienceResearch/BioinformaticsTools/MicroarrayQualityControlProject/default.htm.
34. Wang H, Ach RA, Curry B (2007) Direct and sensitive miRNA profiling from low-input total RNA. Rna 13: 151–159.
35. Lodes MJ, Caraballo M, Suciu D, Munro S, Kumar A, et al. (2009) Detection of cancer with serum miRNAs on an oligonucleotide microarray. PLoS One 4: e6229.

Supplemental description

MicroRNA Profile Predicts Recurrence After Resection in Patients with Hepatocellular Carcinoma within the Milan Criteria.

Fumiaki Sato[1], Etsuro Hatano[2], Koji Kitamura[2], Akira Myomoto[3,4], Takeshi Fujiwara[1], Satoko Takizawa[3], Soken Tsuchiya[1], Gozoh Tsujimoto[4], Shinji Uemoto[2], Kazuharu Shimizu[1]
Affiliation
1: Department of Nanobio Drug Discovery, Graduate School of Pharmaceutical Sciences, Kyoto University, Kyoto, Japan.
2: Department of Hepato-Biliary-Pancreatic Surgery & Transplantation, Kyoto University Hospital, Kyoto, Japan.
3: New Frontiers Research Laboratories, Toray Industries Inc., Kanagawa, Japan.
4: Department of Pharmacogenomics, Graduate School of Pharmaceutical Sciences, Kyoto University, Kyoto, Japan.

Analytical procedures

1. Dataset preparation

The clinical dataset consisted of the 63 clinicopathological information points listed in Table S1. In total, 146 microRNA expression datasheets of both tumor and non-tumor tissues were obtained from the 73 patients. The microRNA expression data was log2 transformed, and normalized by a quantile normalization method [1]. Next, the microRNA expression datasheets of the tumor and non-tumor tissues, and the T/N ratio was concatenated. Since Toray's microRNA microarray chip (the miRBase version 12) contains 866 human microRNA probes, the generated master datasheet consisted of 73 rows and 2598 (=866×3) columns.

2. Filtering of variables

In general, poorly expressed microRNAs tend to have a less repressive impact on biological functions, as compared with highly expressed microRNAs. Therefore, the low expressed microRNAs throughout the samples were excluded from this analysis. The filtering criteria were as follows; if the 75%tile values of a log2 expression of a microRNA did not exceed 6 both in tumor and non-tumor samples, then the microRNA was excluded.

3. Overview of whole microRNA expression profile and unsupervised clustergram.

Supplementary Figure 1 illustrates a heatmap of the microRNA expression in the HCC tumor and non-tumor tissue specimens. The tumor-derived microRNAs profile and non-tumor derived microRNAs profile are almost separated. This finding indicates that this microRNA profiling techniques is working properly in this study.

4. Construction and validation of recurrence-free survival prediction models

A flow chart of the prediction model construction and validation is illustrated in Figure 1. We used a leave-one-out closs-validation method. In each leave-one-out cycle, one patient data was separated from the dataset as test data, and the remaining data were used as a training dataset. Individual microRNA datasets or principal component analysis datasets were the subjects for the next univariate Cox proportional hazard model. According to p-values of the univariate Cox analysis, individual microRNAs or principal components (PC) were prioritized. Using a different number of variables (ranging 1 to 30 variables), a multivariate Cox proportional hazard model was trained. Next, the predicted hazard ratio and predicted survival curve were calculated using the saved test data and a baseline survival curve of the training dataset. The best predictive model was determined by time-averaged AUROC, as described below.

5. Time-averaged AUROCs

The Cox proportional hazard model can analyze data containing censored cases, and can predict survival curves of test cases using a baseline survival curve and predicted hazard ratios. However, it is difficult to evaluate the prediction accuracy of this Cox proportional hazard model. Usually, analysts stratify patients according to Cox model predictions and compare difference between the groups using generalized-Wilcoxon or log-rank tests, or calculate the sensitivity, specificity, or area under the Receiver Operator Characteristic curve (AUROC) at a given time point, such as the 2-year survival, using the predictions and outcomes of patients relevant for the time point. However, the prediction efficiency of these analyses depend upon the stratification method of the patients and the selection of a prediction time point. Therefore, we proposed a new evaluation index for the survival prediction efficiency of the Cox proportional hazard model, i.e. the time-averaged AUROC. The time-averaged AUROC ($\overline{AUROC}$) is defined as below:

$$\overline{AUROC} = \frac{1}{T2 - T1}\int_{T1}^{T2} AUROC(t)dt$$

where *AUROC(t)* represents the AUROC at a fixed time point for patients, and T1 and T2 represent the starting and ending time points for the time-averaging. In a general clinical setting, the distribution of the logarithmic value of the survival time is more closely related to a normal distribution than to the distribution of the original survival time. Therefore, we used the log2 value of the survival time for the $\overline{AUROC}$ calculation in this study.

The difference of the $\overline{AUROC}$ values between the two models was assessed by a paired T-test using AUROC data during the given period from T1 and T2.

The statistical significance of the decreasing or increasing tendency of the AUROCs in the given time period was assessed by Pearson's correlation analysis.

6. Permutation analysis and calculation of false discovery rate.

Table 2 lists HCC recurrence-related microRNAs. To generate this table, we repeated univariate Cox proportional hazard model analysis 386 times (=193 T-miRs + 193 N-miRs). In the case of a multiple-testing procedure, results with low p-values can be obtained by chance. Therefore, we estimated false discovery rate (FDR) by permutation analysis technique. Outcome dataset (consisting of recurrence-free survival and censoring information) was permutated randomly. Using this permutated outcome data and original microRNA expression dataset, we performed univariate Cox proportional hazard model analysis for all 193 T- and 193 N-miRs. We repeated this permutated analysis 1000 times, and obtained a set (S_i) of 1000 p-values for each i-th ranked microRNA (i = 1~193). Then, the FDR of i-th ranked microRNA was defined as (number of p-values in the S_i < the original p-value of the i-th ranked microRNA)/1000.

7. Contribution analysis of each microRNA in the Cox proportional hazard model with principal component analysis (PCA) data

In the Cox analysis using PCA data, the β values for each principal component are provided below:

$$\frac{h(t)}{h_0(t)} = \exp\left(b_1PC_1 + b_2PC_2 + \cdots + b_jPC_j + \cdots + b_nPC_n\right)$$

where h(t) and ho(t) represent the hazard at a given time point 't' for subject case and

baseline survival curve, respectively, and b_j and PC_j are the β values of the j-th principal component (PC). On the other hand, each PC can be expressed as:

$$PC_j = Cj_1 miR_1 + Cj_2 miR_2 + \cdots + Cj_i miR_i + \cdots + Cj_m miR_m$$

where PC_j, Cj_i and miR_i represent the j-th PC, the coefficient of the i-th microRNA in the j-th PC, and the centered expression values of the i-th microRNA, respectively.
Thus, the natural logarithmic value of hazard ratio can be expressed as below:

$$\ln\frac{h(t)}{h_0(t)} = b_1 PC_1 + b_2 PC_2 + \cdots + b_n PC_n$$

$$= \begin{array}{cccc} PC_1 & PC_2 & PC_j & PC_n \\ b_1C1_1miR_1 + & b_2C2_1miR_1 + \cdots + & b_jCj_1miR_1 + \cdots + & b_nCn_1miR_1 + \cdots \\ b_1C1_2miR_2 + & b_2C2_2miR_2 + \cdots + & b_jCj_2miR_2 + \cdots + & b_nCn_2miR_2 + \cdots \\ & \cdots & \cdots & \\ b_1C1_imiR_i + & b_2C2_imiR_i + \cdots + & b_jCj_imiR_i + \cdots + & b_nCn_imiR_i + \cdots \\ & \cdots & \cdots & \\ b_1C1_mmiR_m + & b_2C2_mmiR_m + \cdots + & b_jCj_mmiR_m + \cdots + & b_nCn_mmiR_m \end{array}$$

$$= miR_1 \left(b_1C1_1 + b_2C2_1 + \cdots + b_jCj_1 + \cdots + b_nCn_1\right) + \cdots$$
$$miR_2 \left(b_1C1_2 + b_2C2_2 + \cdots + b_jCj_2 + \cdots + b_nCn_2\right) + \cdots$$
$$\cdots$$
$$miR_i \left(b_1C1_i + b_2C2_i + \cdots + b_jCj_i + \cdots + b_nCn_i\right) + \cdots$$
$$\cdots$$
$$miR_m \left(b_1C1_m + b_2C2_m + \cdots + b_jCj_m + \cdots + b_nCn_m\right)$$

$$= \sum_i^m \left(miR_i \times \left(\sum_j^n b_j Cj_i \right) \right)$$

where m and n represent the number of microRNA and PCs.
Therefore, the contribution of the i-th microRNA can be expressed as: $\sum_j^n b_j Cj_i$.
To estimate 95% confidence interval (CI) of these coefficients, we utilized a case-resampling bootstrap technique. In the construction procedures of the prediction model, a resampled dataset was generated from the PCA data, and coefficients, $\sum_j^n b_j Cj_i$, were calculated using the resampled dataset. This bootstrap step were repeated 1000 times. The 95% CI was defined as an interval between 2.5 and 97.5 percentile of 1000 coefficients generated by this bootstrap resampling procedure.

8. mRNA expression profiling by DNA chip

For the DNA microarray analysis, 400 ng of total RNA was amplified and labeled using an TargetAmp™ 1-Round Aminoallyl-aRNA Amplification Kit (Epicentre, Madison, WI) according to the manufacturer's instructions. Each non-tumor sample of aRNA labeled with Cy3 and tumor aRNA labeled with Cy5 were cohybridized with 3D-Gene™ Human 25K (Toray Industries, Inc., Tokyo, Japan) at 37℃ for 16 h. After hybridization, each DNA chip

was washed and dried in an ozone-free booth. Hybridization signals derived from Cy3 and Cy5 were scanned using Scan Array Express (PerkinElmer, Waltham, MA). The scanned image was analyzed using GenePix Pro (Molecular Devices, Sunnyvale, CA). All the analyzed data were scaled by quantile normalization.

9. Screening and ontology information of putative target genes of miR-96

MicroRNAs regulate gene expression post-transcriptionally by repressing translation of protein synthesis and inducing degradation of target mRNA. Therefore, the expression level of mRNA regulated by the latter mechanism is supposed to be inversely correlated with the microRNA expression level. In order to identify the putative target genes of miR-96, we screened mRNAs that are inversely correlated to miR-96 expression level in 146 samples (tumor and non-tumor paired samples derived from 73 patients), and that have microRNA target sites predicted by Target Scan v.5.1 (http://www.targetscan.org/) in their 3'-UTR. A list of putative miR-96 with p-values less than 0.01 are shown in Table S9-12. In addition, ontology information of each screened target gene is retrieved from the NCBI Entrez site (http://www.ncbi.nlm.nih.gov/gene), and provided in Table S9-12. We provide mRNA expression dataset consisting of 787 mRNAs that are identified as putative target genes of miR-96 by the Target Scan, in a Microsoft Excel file format (Table S13).

References

1. Bolstad BM, Irizarry RA, Astrand M, Speed TP (2003) A comparison of normalization methods for high density oligonucleotide array data based on variance and bias. Bioinformatics 19: 185-193.

Figure S1

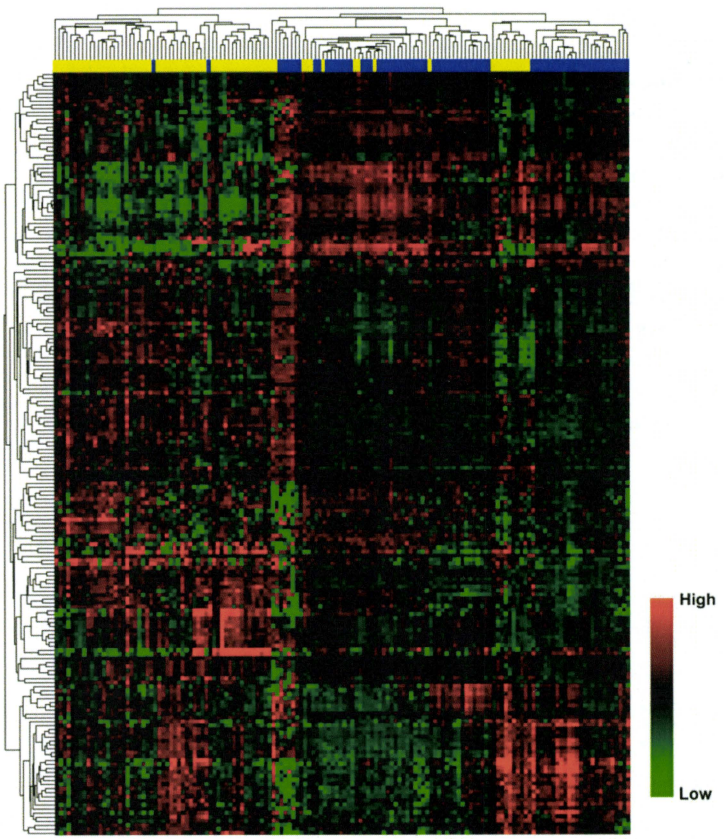

Figure S2

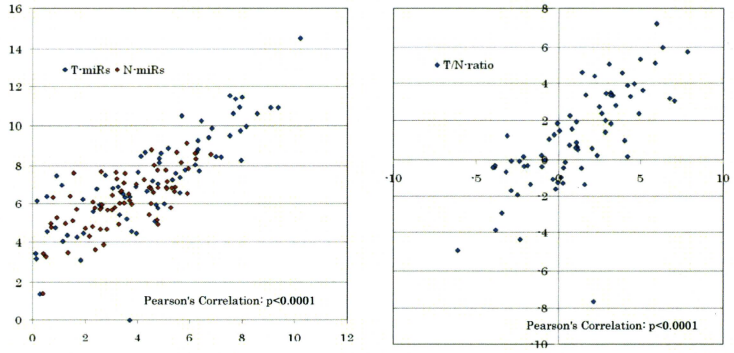
T-miRs
N-miRs
Pearson's Correlation: p<0.0001
T/N-ratio
Pearson's Correlation: p<0.0001

Table S1

Variables in clinicopathological dataset (n=63)			
1	age	33	invasion to serosa*
2	gender	34	no co-existing liver disease**
3	ICG R15	35	co-existing liver disease (chronic hepatitis)**§
4	ICG k	36	co-existing liver disease (liver cirrhosis)**§
5	clinical stage*	37	co-existing liver disease (others)**§
6	Child-Pugh points	38	T-factor*
7	Child-Pugh classification	39	Hr-factor (hepatic resection)*
8	serum, AST	40	resected other organs
9	serum, ALT	41	curability
10	blood, platelet	42	macroscopic morphology
11	serum, total-bilirubin	43	capsule formation
12	serum, direct-bilirubin	44	infiltration into capsule
13	serum, albmin	45	septum formation
14	prothrombin activity	46	intrahepatic metastasis
15	prothrombin time	47	vessel invasion
16	alpha feto protein (log10 transformed)	48	surgical mergin
17	PIVKA (log10 transformed)	49	postoperative complication
18	hepatitis B Virus Antigen	50	# of tumor¶
19	hapatitis C Virus Antibody	51	capsule formation ¶
20	intraoperative hemorrhage	52	infiltration into capsule ¶
21	operation time	53	septum formation ¶
22	multiplicity of tumor	54	vessel invasion ¶
23	# of tumors §	55	intrahepatic metastasis ¶
24	longest diameter of tumor§	56	pathological tumor grade
25	length of minor axis of tumor §	57	co-existing liver disease (chronic hepatitis)**¶
26	tumor location (anterior segment)**	58	co-existing liver disease (liver cirrhosis)**¶
27	tumor location (posterior segment)**	59	co-existing liver disease (others)**¶
28	tumor location (medial segment)**	60	grade of chronic hepatitis ¶†
29	tumor location (lateral segment)**	61	stage of chronic hepatitis ¶†
30	tumor location (caudate segment)**	62	T-facor*¶
31	longest diameter of resected tumor	63	curability*¶
32	H-factor*		

*: the 4th Japanese Guideline for HCC[1]
**: dummy variables
§:clinical diagnosis
¶:pathological diagnosis
†: new Inuyama classification (1996)[2]

1. Liver Cancer Study Group of Japan a (2000) The General Rules for the Clinical and Pathological Study of Primary Liver Cancer. Tokyo: Kanehara & Co., Ltd.
2. Ichida F, Tsuji T, Omata M, Ichida T, Inoue K, et al. (1996) New Inuyama Classification; new criteria for histological assessment of chronic hepatitis. International Hepatology Communications 6: 112-119.

Table S2

Target gene	Gene name	context score*	Aggregate P_{CT}*	Rank**	correlation coefficient†	p-value†	Gene Ontology function	Gene Ontology Process	Pubmed hit count‡
TAF15	TAF15 RNA polymerase II, TATA box binding protein (TBP)-associated factor	-0.24	0.73	337	-0.3977	0.000001	nucleotide binding		0
LRP6	low density lipoprotein receptor-related protein 6	-0.2	0.74	419	-0.3872	0.000001	low-density lipoprotein receptor activity Wnt-protein binding	negative regulation of Wnt receptor signaling pathway	4
FOXO1	forkhead box O1	-0.6	0.95	28	-0.3347	0.000036	sequence-specific DNA binding transcription factor activity	regulation of cell proliferation	43
ACADSB	acyl-Coenzyme A dehydrogenase, short/branched chain	-0.1	0.69	675	-0.3331	0.000040	acyl-CoA dehydrogenase activity	lipid metabolic process	0
MAP2K1	mitogen-activated protein kinase kinase 1	-0.23	0.8	354	-0.3317	0.000043	MAP kinase kinase activity Ras GTPase binding	cell motility negative regulation of cell proliferation	22
INTS6	integrator complex subunit 6	-0.21	0.74	395	-0.3132	0.000118	transmembrane receptor activity	snRNA processing	1
TAPT1	transmembrane anterior posterior transformation 1	-0.21	0.74	395	-0.2774	0.000701	growth hormone-releasing hormone receptor activity	embryonic skeletal system development	0
EPB41L4B	erythrocyte membrane protein band 4.1 like 4B	-0.2	0.83	419	-0.2733	0.000844	cytoskeletal protein binding		0
CADM2	cell adhesion molecule 2	-0.16	0.69	552	-0.2686	0.001047			0
SEC14L2	SEC14-like 2 (S. cerevisiae)	-0.22	0.59	374	-0.2680	0.001072	phospholipid binding vitamin E binding	positive regulation of cholesterol biosynthetic process	6
UNC13C	unc-13 homolog C (C. elegans)	-0.8	0.94	6	-0.2679	0.001076	metal ion binding	Exocytosis, synaptic transmission	0
CREB3L2	cAMP responsive element binding protein 3-like 2	-0.42	0.71	119	-0.2667	0.001139	cAMP response element binding transcription factor activity		0
ETNK2	ethanolamine kinase 2	-0.08	0.74	714	-0.2662	0.001164	ethanolamine kinase activity	placenta development	0
PIK3R1	phosphoinositide-3-kinase, regulatory subunit 1 (alpha)	-0.28	0.74	259	-0.2655	0.001201	ErbB-3 class receptor binding phosphoinositide 3-kinase regulator activity	positive regulation of glucose import insulin receptor signaling pathway	1
CLIC5	chloride intracellular channel 5	-0.05	0.74	745	-0.2517	0.002177	voltage-gated chloride channel activity	chloride transport	0
ELL2	elongation factor, RNA polymerase II, 2	-0.17	0.74	510	-0.2497	0.002369	RNA polymerase II transcription elongation factor activity	regulation of transcription	0
EGR3	early growth response 3	-0.17	0.74	510	-0.2493	0.002414	sequence-specific DNA binding transcription factor activity	circadian rhythm peripheral nervous system development	1
GPM6A	glycoprotein M6A	-0.27	0.6	276	-0.2486	0.002482	calcium channel activity		0
REV1	REV1 homolog (S. cerevisiae)	-0.52	0.95	50	-0.2481	0.002530	damaged DNA binding	DNA repair	0
SLC1A2	solute carrier family 1 (glial high affinity glutamate transporter), member 2	-0.32	0.74	210	-0.2461	0.002753	L-glutamate transmembrane transporter activity	synaptic transmission	0
LUZP1	leucine zipper protein 1	-0.21	0.81	395	-0.2440	0.002994			0
TMEM145	transmembrane protein 145	-0.17	0.74	510	-0.2431	0.003110			0
GPHN	gephyrin	-0.35	0.66	172	-0.2344	0.004410	nucleotidyltransferase activity	Mo-molybdopterin cofactor biosynthetic process	0
ERLIN1	ER lipid raft associated 1	-0.35	0.72	172	-0.2325	0.004751		ER-associated protein catabolic process	0
ANKRD52	ankyrin repeat domain 52	-0.25	0.86	311	-0.2322	0.004795			0
CUL4A	cullin 4A	-0.04	0.72	755	-0.2300	0.005233	ubiquitin protein ligase binding	DNA repair, cell cycle arrest	2
FAM13A1	family with sequence similarity 13, member A1	-0.17	0.7	510	-0.2276	0.005729	GTPase activator activity	signal transduction	0
SCML4	sex comb on midleg-like 4 (Drosophila)	-0.21	0.66	395	-0.2252	0.006270	DNA binding	regulation of transcription	0
SYT9	synaptotagmin IX	-0.22	0.28	374	-0.2241	0.006544	transporter activity	regulation of calcium ion-dependent exocytosis, regulation of insulin secretion	0
IRS1	insulin receptor substrate 1	-0.24	0.61	337	-0.2229	0.006841	insulin-like growth factor receptor binding phosphoinositide 3-kinase binding	insulin-like growth factor receptor signaling pathway, PI3-kinase cascade, positive regulation of cell proliferation	92
TSKU	tsukushin	-0.26	0.79	294	-0.2227	0.006893	protein binding		0
SMCR8	Smith-Magenis syndrome chromosome region, candidate 8	-0.12	0.74	636	-0.2197	0.007719			0
GJA3	gap junction protein, alpha 3, 46kDa	-0.16	0.74	552	-0.2181	0.008172	gap junction channel activity	cell-cell signaling	0

Table S3

miR name	T-miRs	N-miRs	fold-change	p-value
miR-224	7.1005	5.8716	2.3439	0.00006
miR-221	8.9564	7.7724	2.2721	<0.00001
miR-96	4.5990	3.4966	2.1470	0.00302
miR-130b	6.6031	5.5227	2.1146	<0.00001
miR-452	5.7578	4.9143	1.7944	0.00259
miR-106b	9.8617	9.0395	1.7681	<0.00001
miR-222	7.3771	6.5574	1.7651	<0.00001
miR-21	12.0351	11.2189	1.7608	<0.00001
miR-18b	5.6000	4.8291	1.7064	0.00248
miR-93	8.6849	7.9448	1.6703	<0.00001
miR-425	8.0632	7.3283	1.6643	<0.00001
miR-1268	8.7846	8.0725	1.6381	<0.00001
miR-675	6.0331	5.3300	1.6280	0.00033
miR-1469	9.1517	8.4493	1.6272	0.00001
miR-1228*	9.7963	9.1177	1.6006	<0.00001
miR-18a	5.9948	5.3167	1.6001	0.00841
miR-664	8.2808	7.6315	1.5684	<0.00001
miR-1915	7.3535	6.7203	1.5510	0.00016
miR-362-3p	5.4439	4.8225	1.5384	0.00398
miR-301a	6.7046	6.0914	1.5297	0.00444
miR-663	9.8008	9.1948	1.5221	0.00066
miR-34a	9.6314	9.0273	1.5201	0.00001
miR-660	6.8796	6.2846	1.5104	0.00016
miR-193b	8.9301	8.3360	1.5095	0.00014
miR-151-5p	8.9698	8.4085	1.4756	0.00003
miR-25	8.9278	8.3846	1.4572	<0.00001
miR-1909	7.1333	6.5913	1.4560	0.00001
miR-494	9.7928	9.3206	1.3872	0.00023
miR-638	10.4487	9.9916	1.3728	0.00023
miR-17	9.8009	9.3496	1.3673	0.00176
miR-107	10.9199	10.5205	1.3190	<0.00001
miR-365	8.1769	7.7796	1.3170	0.00150
miR-151-3p	7.1208	6.7503	1.2928	0.00196
miR-191	10.3609	9.9908	1.2924	<0.00001
miR-103	11.1865	10.8314	1.2791	0.00059
miR-140-3p	8.3389	8.0014	1.2635	0.00015
miR-185	7.7581	7.4236	1.2609	0.00318
miR-361-5p	8.0541	7.7214	1.2594	0.00004
miR-15a	8.7356	8.4428	1.2250	0.00068
miR-320a	8.1341	7.8845	1.1888	0.00792
miR-29a	11.1116	10.9187	1.1430	0.00739
miR-1826	14.6080	14.4679	1.1020	0.00303

Table S4

miR name	T-miR	N-miR	fold-change	p-value
miR-200a	5.8183	8.5496	0.1506	<0.00001
miR-375	3.7664	6.0955	0.1990	<0.00001
miR-200b	6.7698	9.0919	0.2000	<0.00001
miR-199b-3p	8.6670	10.8304	0.2232	<0.00001
miR-199a-3p	8.7558	10.8862	0.2284	<0.00001
miR-199a-5p	8.5426	10.5858	0.2426	<0.00001
miR-150	6.0219	7.7215	0.3079	<0.00001
miR-10a	6.8784	8.4695	0.3319	<0.00001
miR-424	6.8159	8.3325	0.3495	<0.00001
miR-214	6.9813	8.4080	0.3720	<0.00001
miR-139-5p	4.8902	6.3078	0.3744	<0.00001
miR-451	11.4110	12.7522	0.3947	<0.00001
miR-142-3p	4.3882	5.5899	0.4348	0.00001
miR-142-5p	6.7147	7.8031	0.4703	0.00003
miR-223	8.3237	9.3963	0.4755	<0.00001
miR-146a	6.4679	7.5048	0.4874	0.00001
miR-486-5p	4.9461	5.9425	0.5012	<0.00001
miR-30a*	6.1348	7.1145	0.5071	<0.00001
miR-130a	8.2858	9.2523	0.5118	<0.00001
miR-376c	4.9713	5.8816	0.5321	0.00542
miR-378	8.3006	9.1927	0.5388	<0.00001
miR-125a-5p	8.1841	9.0551	0.5468	<0.00001
miR-195	8.8553	9.7022	0.5560	<0.00001
miR-497	7.3460	8.1444	0.5750	0.00002
miR-422a	7.1003	7.8778	0.5834	<0.00001
miR-342-3p	8.0099	8.6998	0.6199	<0.00001
miR-125b	10.3309	10.9920	0.6324	0.00001
miR-101	6.4174	7.0780	0.6326	0.00005
miR-1249	4.6112	5.2266	0.6527	0.00728
miR-30e*	7.7371	8.3455	0.6559	<0.00001
miR-1238	5.1302	5.7055	0.6711	0.00216
miR-335	6.6345	7.1763	0.6869	0.00812
miR-145	9.6902	10.2310	0.6874	0.00037
miR-455-5p	6.0197	6.5470	0.6939	0.00087
miR-22*	5.4614	5.9578	0.7089	0.00632
miR-99a	10.4387	10.9317	0.7105	0.00047
miR-146b-5p	9.6150	10.0391	0.7453	0.00990
miR-100	10.4659	10.8843	0.7482	0.00039
miR-143	10.8380	11.2255	0.7645	0.00411
let-7g	11.0311	11.4135	0.7672	0.00078
miR-181a	7.5643	7.9462	0.7674	0.00515
miR-99b	7.5207	7.8866	0.7760	0.00058
miR-22	12.1227	12.4560	0.7937	0.00006
miR-30a	10.4827	10.8113	0.7963	0.00034
miR-26a	12.3555	12.6796	0.7988	0.00004
miR-30c	10.9891	11.2535	0.8325	0.00007
let-7c	11.5850	11.8016	0.8606	0.00070
let-7a	12.2072	12.3928	0.8793	0.00395
miR-1280	14.0985	14.2756	0.8845	0.00168

Table S5

miR name	T-miRs	normal	fold-change	p-value	miR name	N-miRs	normal	fold-change	p-value
Up-regulated miRs									
miR-96	4.5990	1.8477	6.7330	0.03489	miR-96	3.4966	1.8477	3.1359	0.04947
miR-222	7.3771	5.1257	4.7614	0.00001	miR-222	6.5574	5.1257	2.6976	0.00939
miR-18b	5.6000	3.4268	4.5102	0.03660	miR-886-3p	7.7848	6.5724	2.3173	0.04503
miR-224	7.1005	5.1620	3.8330	0.04204	miR-146b-5p	10.0391	9.0101	2.0406	0.00038
miR-221	8.9564	7.3352	3.0763	0.00010	miR-199a-3p	10.8862	10.1048	1.7188	0.01696
miR-21	12.0351	10.4628	2.9737	0.00007	miR-181a	7.9462	7.1682	1.7147	0.00651
miR-1469	9.1517	7.7425	2.6558	0.00302	miR-199a-5p	10.5858	9.8103	1.7118	0.01517
miR-362-3p	5.4439	4.1095	2.5217	0.04277	miR-199b-3p	10.8304	10.1247	1.6309	0.02380
miR-663	9.8008	8.5582	2.3663	0.01236	miR-10a	8.4695	7.7943	1.5969	0.03236
miR-106b	9.8617	8.6820	2.2654	0.00023	miR-214	8.4080	7.7728	1.5531	0.03594
miR-34a	9.6314	8.4736	2.2312	0.01399					
miR-25	8.9278	8.2994	1.5459	0.03904					
Down-regulated miRs									
miR-375	3.7664	6.2964	0.1731	0.01715	miR-1238	5.7055	7.0204	0.4020	0.00922
miR-1249	4.6112	6.6075	0.2506	0.00533	miR-296-5p	8.4425	9.6868	0.4221	0.01721
miR-139-5p	4.8902	6.8648	0.2544	0.01140	miR-1228	6.0568	7.1856	0.4573	0.02378
miR-1238	5.1302	7.0204	0.2698	0.00990	miR-1913	8.3088	9.2908	0.5063	0.00631
miR-625*	5.3830	7.0589	0.3130	0.00344	miR-940	6.9842	7.8839	0.5360	0.02220
miR-422a	7.1003	8.7371	0.3216	0.00783	miR-422a	7.8778	8.7371	0.5512	0.01481
miR-486-5p	4.9461	6.4846	0.3442	0.02208	miR-148a	10.3720	11.1663	0.5766	0.03234
miR-378	8.3006	9.8241	0.3478	0.00364	miR-193a-5p	5.7622	6.5466	0.5806	0.02435
miR-296-5p	8.2098	9.6868	0.3592	0.00125	miR-365	7.7796	8.5251	0.5965	0.01594
miR-101	6.4174	7.7477	0.3977	0.01811	miR-101	7.0780	7.7477	0.6286	0.04963
miR-1228	5.9237	7.1856	0.4170	0.01134	miR-1201	9.0958	9.7294	0.6446	0.04848
miR-1913	8.1404	9.2908	0.4505	0.00105	miR-92a	8.5022	8.9180	0.7496	0.04124
miR-193a-5p	5.4028	6.5466	0.4526	0.02306					
miR-30e*	7.7371	8.5683	0.5620	0.04295					
miR-125a-3p	7.5449	8.2814	0.6002	0.04314					

Table S6

	T-miR					N-miR			
miR	HBV(+)	HBV(-)	Diff	p-value*	miR	HBV(+)	HBV(-)	Diff	p-value*
Up-regulated					Up-regulated				
miR-106b	10.3206	9.7715	0.5491	0.0034	miR-24	11.6927	11.5276	0.1651	0.0435
miR-18a	7.4176	5.7149	1.7026	0.0053					
miR-18b	6.9740	5.3297	1.6443	0.0082					
miR-19b	12.0658	11.4107	0.6551	0.0126					
miR-483-3p	6.0029	3.9654	2.0375	0.0157					
miR-92a	9.0847	8.4392	0.6455	0.0167					
miR-19a	10.0270	9.3212	0.7057	0.0195					
miR-146a	7.3693	6.2906	1.0786	0.0298					
miR-375	4.9232	3.5388	1.3844	0.0320					
miR-483-5p	6.3649	4.7003	1.6646	0.0368					
miR-25	9.2463	8.8651	0.3812	0.0408					
miR-320a	8.5294	8.0563	0.4731	0.0484					
miR-96	5.9103	4.3410	1.5692	0.0494					
Down-regulated					Down-regulated				
miR-34b*	4.7227	6.3285	-1.6058	0.0001	miR-204	5.0377	5.8588	-0.8211	0.0035
miR-99b	6.8002	7.6624	-0.8622	0.0006	miR-186	4.9359	5.8206	-0.8847	0.0045
miR-29b	8.9477	9.5701	-0.6223	0.0018	miR-320a	7.5878	7.9429	-0.3550	0.0047
miR-125b	9.3161	10.5306	-1.2145	0.0019	miR-335	6.3978	7.3294	-0.9316	0.0106
miR-99a	9.6034	10.6030	-0.9996	0.0024	miR-486-5p	5.3699	6.0552	-0.6853	0.0121
miR-100	9.7506	10.6066	-0.8560	0.0029	miR-320b	7.6168	7.8877	-0.2709	0.0215
miR-34a	8.9715	9.7613	-0.7898	0.0052	miR-101	6.6977	7.1528	-0.4551	0.0282
miR-365	7.4817	8.3136	-0.8319	0.0052	miR-374a	5.2447	5.8441	-0.5994	0.0294
miR-30e*	7.1643	7.8498	-0.6855	0.0059	miR-361-5p	7.5175	7.7615	-0.2439	0.0305
miR-29c	8.8776	9.5295	-0.6519	0.0102	miR-30e*	8.0976	8.3943	-0.2967	0.0326
miR-193b	8.1940	9.0749	-0.8809	0.0139	miR-28-5p	7.9896	8.5349	-0.5453	0.0366
miR-30a	10.0684	10.5642	-0.4958	0.0156	miR-20a	8.4863	9.2370	-0.7506	0.0381
miR-374b	4.2973	5.4034	-1.1061	0.0201	miR-452	4.2277	5.0494	-0.8217	0.0405
miR-195	8.1499	8.9941	-0.8442	0.0232	miR-126*	6.1436	6.9171	-0.7734	0.0406
miR-362-3p	4.7253	5.5853	-0.8600	0.0290	miR-193a-5p	5.4007	5.8333	-0.4325	0.0425
miR-26b	9.7553	10.2310	-0.4756	0.0306	miR-30a*	6.8183	7.1728	-0.3545	0.0496
miR-361-3p	6.1658	6.6966	-0.5309	0.0319					
miR-192*	4.3472	5.3080	-0.9608	0.0373					
miR-660	6.3082	6.9920	-0.6839	0.0414					
miR-374a	5.0107	5.6917	-0.6810	0.0419					
miR-125a-5p	7.6032	8.2983	-0.6951	0.0485					

Table S7

	T-miR					N-miR			
miR	HCV(+)	HCV(-)	Diff	p-value*	miR	HCV(+)	HCV(-)	Difference	p-value*
Up-regulated					Up-regulated				
miR-34b*	6.4265	5.2253	1.2012	0.0003	miR-222	6.8848	5.7984	1.0864	<0.0001
miR-30e*	7.9329	7.2832	0.6497	0.0011	miR-150	8.0739	6.9044	1.1695	<0.0001
miR-192*	5.4894	4.3634	1.1260	0.0021	let-7i	9.2825	8.9220	0.3604	0.0008
miR-455-3p	8.6178	8.0202	0.5977	0.0036	miR-181a	8.0824	7.6304	0.4519	0.0008
miR-193b	9.1567	8.4048	0.7519	0.0092	miR-886-3p	8.0565	7.1551	0.9014	0.0016
miR-215	9.5249	8.9718	0.5531	0.0167	miR-96	3.8601	2.6540	1.2061	0.0030
miR-34a	9.7944	9.2538	0.5406	0.0187	miR-106b	9.1893	8.6924	0.4969	0.0032
miR-30a	10.6001	10.2103	0.3898	0.0188	miR-155	5.7522	4.6028	1.1494	0.0033
miR-365	8.3473	7.7817	0.5656	0.0196	miR-342-3p	8.8314	8.3948	0.4366	0.0033
miR-125a-3p	7.6574	7.2840	0.3735	0.0353	miR-142-5p	8.0579	7.2124	0.8455	0.0048
miR-30c	11.0656	10.8115	0.2541	0.0463	miR-199a-5p	10.7131	10.2907	0.4224	0.0060
miR-26b	10.2583	9.9081	0.3502	0.0494	miR-221	7.9253	7.4180	0.5073	0.0073
					miR-199b-3p	10.9496	10.5542	0.3954	0.0090
					miR-146b-5p	10.1462	9.7907	0.3555	0.0093
					miR-142-3p	5.8838	4.9084	0.9755	0.0102
					miR-362-3p	5.0836	4.2171	0.8665	0.0110
					miR-199a-3p	11.0069	10.6066	0.4003	0.0116
					miR-331-3p	6.3914	5.8842	0.5072	0.0233
					let-7d	12.1539	11.9643	0.1897	0.0267
					miR-16	11.2669	11.0684	0.1985	0.0288
					miR-186	5.8385	5.2965	0.5420	0.0334
					miR-147	5.5457	5.0445	0.5012	0.0406
					miR-140-3p	8.0675	7.8483	0.2191	0.0414
					miR-185	7.5071	7.2301	0.2770	0.0432
					miR-146a	7.6435	7.1835	0.4600	0.0459
Down-regulated					Down-regulated				
miR-146a	6.1684	7.1622	-0.9938	0.0127	miR-296-5p	8.1440	9.1344	-0.9904	<0.0001
miR-24	11.4161	11.6670	-0.2509	0.0161	miR-1913	8.1286	8.7266	-0.5980	0.0004
miR-370	4.9433	5.7049	-0.7615	0.0178	miR-148a	10.1907	10.7925	-0.6019	0.0008
miR-23a	11.8544	12.1104	-0.2560	0.0240	miR-422a	7.7153	8.2547	-0.5394	0.0014
miR-744	7.2950	7.8370	-0.5420	0.0369	miR-1228	5.8350	6.5709	-0.7359	0.0022
miR-1228*	9.6644	10.1021	-0.4377	0.0389	miR-1238	5.4915	6.2016	-0.7101	0.0034
miR-494	9.6574	10.1067	-0.4493	0.0461	miR-1201	8.9610	9.4083	-0.4473	0.0039
miR-575	6.1797	6.6792	-0.4995	0.0493	miR-99a	10.8449	11.1329	-0.2880	0.0068
					miR-625*	5.5356	6.3972	-0.8615	0.0070
					miR-365	7.6609	8.0547	-0.3939	0.0081
					miR-940	6.8369	7.3257	-0.4888	0.0104
					miR-1249	4.9838	5.7895	-0.8058	0.0207
					miR-378	9.0651	9.4886	-0.4235	0.0232
					miR-92a	8.4412	8.6436	-0.2024	0.0420

Table S8

	T-miRs						
miR name	grade1	grade2	grade3	diff (1 vs 2)	diff (1 vs 3)	diff (2 vs 3)	p-value*
miR-191	10.1177	10.5007	10.1918	-0.3831	-0.0742	0.3089	0.0039
miR-126*	7.4668	6.5014	6.3017	0.9654	1.1651	0.1998	0.0074
miR-1915	7.6699	7.3598	6.3638	0.3101	1.3061	0.9960	0.0202
miR-378	8.7756	8.0561	8.4477	0.7194	0.3279	-0.3915	0.0217
miR-455-5p	6.2626	6.0735	4.9452	0.1891	1.3175	1.1284	0.0232
miR-126	12.0775	11.6789	11.7130	0.3985	0.3644	-0.0341	0.0234
miR-486-3p	7.0058	6.4565	5.6443	0.5493	1.3615	0.8122	0.0285
miR-1228	6.1406	5.9577	5.0541	0.1828	1.0864	0.9036	0.0290
miR-20a	9.3135	9.3725	8.0935	-0.0590	1.2199	1.2790	0.0397
miR-923	13.3713	13.9565	13.5210	-0.5852	-0.1497	0.4355	0.0419
miR-106b	9.5858	9.9831	9.9092	-0.3974	-0.3235	0.0739	0.0425
miR-744	7.8564	7.3688	6.8402	0.4876	1.0162	0.5286	0.0456

Table S9

HBV(+) cases (n=12)

T-miRs				N-miRs			
Rank	microRNA	hazard ratio	p-value	Rank	microRNA	hazard ratio	p-value
1	miR-1913	0.0992	0.0057	1	miR-638	0.1125	0.0073
2	miR-663	0.2277	0.0069	2	miR-1202	0.6105	0.0112
3	miR-1909	0.1647	0.0106	3	let-7i	18.629	0.0133
4	miR-575	0.2499	0.0140	4	miR-99b	8.4818	0.0140
5	miR-638	0.2146	0.0167	5	miR-107	15.909	0.0159
6	miR-18b	2.1562	0.0205	6	miR-146b-5p	7.3577	0.0184
7	miR-18a	2.2643	0.0215	7	miR-223	5.9927	0.0188
8	miR-1469	0.2768	0.0243	8	miR-663	0.3757	0.0189
9	miR-1908	0.2849	0.0251	9	miR-130b	2.0950	0.0202
10	miR-20a	3.1284	0.0255	10	miR-96	1.7335	0.0206
11	miR-20b	2.7301	0.0267	11	miR-23a	16.157	0.0211
12	miR-455-3p	2.5900	0.0277	12	miR-484	8.7674	0.0218
13	miR-296-5p	0.2116	0.0277	13	miR-146a	4.9436	0.0220
14	miR-362-3p	2.3579	0.0314	14	miR-1909	0.1095	0.0230
15	miR-17	3.4918	0.0343	15	miR-27a	14.401	0.0269
16	miR-106a	3.1753	0.0346	16	miR-149*	0.2075	0.0292
17	miR-335	2.6876	0.0362	17	miR-1260	0.0136	0.0301
18	miR-92a	3.0776	0.0372	18	miR-122*	0.3034	0.0311
19	miR-29a	0.2359	0.0435	19	miR-23b	10.679	0.0320
20	miR-940	0.2839	0.0449	20	miR-192	0.2663	0.0332

Table S10

HCV(+) cases (n=51)							
T-miRs				N-miRs			
Rank	microRNA	hazard ratio	p-value	Rank	microRNA	hazard ratio	p-value
1	miR-100	0.4810	0.0008	1	miR-27a	6.7460	0.0004
2	miR-99a	0.5821	0.0012	2	miR-486-5p	0.4468	0.0008
3	miR-125b	0.5773	0.0048	3	miR-24	13.869	0.0013
4	miR-92b*	1.6247	0.0131	4	miR-96	1.5296	0.0016
5	miR-30c	0.3833	0.0194	5	miR-21	1.6457	0.0026
6	miR-1268	1.6946	0.0200	6	miR-18a	2.2505	0.0038
7	miR-575	1.5276	0.0210	7	miR-142-3p	1.5871	0.0040
8	miR-1275	1.3010	0.0221	8	miR-23a	5.8634	0.0042
9	miR-30e	0.6382	0.0230	9	miR-148a	0.5434	0.0050
10	miR-130b	0.6909	0.0236	10	miR-1238	0.5584	0.0057
11	miR-1246	1.2356	0.0252	11	miR-191	9.1921	0.0105
12	miR-129-5p	0.7183	0.0261	12	miR-222	1.8491	0.0109
13	miR-148b	0.7898	0.0333	13	miR-296-5p	0.5316	0.0116
14	miR-22	0.5544	0.0347	14	miR-103	6.3409	0.0116
15	miR-103	0.6878	0.0375	15	let-7f	6.3824	0.0124
16	miR-99b	0.6843	0.0411	16	miR-18b	1.6347	0.0144
17	miR-638	1.4609	0.0455	17	miR-107	6.1065	0.0173
18	miR-665	1.2995	0.0485	18	miR-30c	0.4300	0.0179
19				19	miR-146b-5p	2.6044	0.0186
20				20	miR-378	0.6372	0.0187

Table S11

HBV(-) HCV(-) cases (n=14)

T-miRs				N-miRs			
Rank	microRNA	hazard ratio	p-value	Rank	microRNA	hazard ratio	p-value
1	miR-17	30.384	0.0080	1	miR-30b	0.0170	0.0071
2	miR-106a	24.516	0.0109	2	miR-342-3p	0.0068	0.0189
3	miR-20a	29.072	0.0139	3	let-7e	32.803	0.0233
4	miR-93	48.859	0.0143	4	miR-147	147.4	0.0235
5	miR-92a	42.274	0.0148	5	miR-152	12.138	0.0249
6	miR-103	17.182	0.0154	6	miR-1202	0.5826	0.0352
7	miR-92b	16.617	0.0186	7	miR-126*	38.122	0.0384
8	miR-125b	0.0234	0.0191	8	miR-128	31.80	0.0389
9	miR-107	17.215	0.0193	9	miR-17	54.282	0.0416
10	miR-24	0.0780	0.0209	10	miR-93	25542	0.0468
11	miR-19a	8.6331	0.0227	11	miR-146a	0.0050	0.0481
12	miR-140-3p	0.0400	0.0230	12	miR-26b	58.694	0.0484
13	miR-20b	63.800	0.0260	13	miR-335	17.668	0.0492
14	miR-483-3p	1.4653	0.0272	14	miR-374b	8.9145	0.0497
15	miR-98	4.3393	0.0349	15			
16	let-7f	1122.9	0.0357	16			
17	miR-224	1.8818	0.0407	17			
18	miR-148b	6.4607	0.0415	18			
19	miR-30e	3.6760	0.0431	19			
20	miR-125a-5p	0.2555	0.0456	20			

Table S12

Grade 1 (well diff, n=21)				Grade 2 (mod diff, n=45)			
Rank	T-miRs	hazard ratio	p-value	Rank	T-miRs	hazard ratio	p-value
1	miR-224	2.1100	0.0049	1	miR-99a	0.5806	0.0007
2	miR-193b	3.3817	0.0074	2	miR-100	0.5640	0.0015
3	miR-152	0.2691	0.0142	3	miR-378	0.6030	0.0092
4	miR-452	1.6740	0.0219	4	miR-30e*	0.5498	0.0186
5	miR-191	0.1882	0.0252	5	miR-129-5p	0.7036	0.0291
6	miR-20a	2.1191	0.0260	6	miR-140-3p	0.5061	0.0300
7	miR-92b	2.0843	0.0270	7	miR-422a	0.7489	0.0352
8	miR-1228	2.1790	0.0288	8	miR-99b	0.6989	0.0406
9	miR-199a-5p	0.6349	0.0298	9	miR-125b	0.8529	0.0468
10	miR-20b	2.0342	0.0325	10	miR-193b	0.7259	0.0493
11	miR-376c	0.7592	0.0372				
12	miR-145	0.3157	0.0438				
13	miR-199b-3p	0.6717	0.0454				